

# Demonstrated $4 \times 4$ Gbps Silicon Photonic Integrated Parallel Electronic to WDM Interface

**Benjamin G. Lee, Benjamin A. Small, Justin D. Foster, and Keren Bergman**

*Department of Electrical Engineering, Columbia University, 500 West 120<sup>th</sup> Street, New York, New York 10027  
benlee@ee.columbia.edu*

**Qianfan Xu and Michal Lipson**

*School of Electrical and Computer Engineering, Cornell University, 411 Phillips Hall, Ithaca, New York 14853*

**Abstract:** A  $4 \times 4$  Gbps microring modulator cascade with the ability to directly convert parallel electrical bus data into multiple-wavelength optical signals in a single silicon-on-insulator waveguide interface is demonstrated with  $< 10^{-12}$  bit error rates.

©2006 Optical Society of America

**OCIS codes:** (130.0250) Optoelectronics; (230.4110) Modulators

## 1. Introduction

In the search for ultrahigh-bandwidth interconnection networks to relieve the communications bottleneck in high performance computing systems (HPCS), the additional capacity supplied by wavelength division multiplexing (WDM) provides a distinct advantage for optical technologies. Photonic integrated circuits (PICs) leverage this advantage, while also realizing low power consumption and low latency as a result of their micron-sized components. Additionally, the ability to integrate many small devices, each with unique functionality, onto a single platform places PICs in an optimal position to be used for board-to-board, chip-to-chip, and intra-chip interconnects. The silicon-on-insulator (SOI) material system has recently been the subject of focused research as a key platform for PICs because of the spatial density afforded by the high index contrast, along with low optical loss and CMOS processing compatibility [1]. SOI-based PICs, therefore, have the potential to realize high-bandwidth interconnects in HPCS networks.

The conversion of the highly parallel electronic data into wavelength-parallel optical signals will be a key component of any PIC implementation. However, it should be performed in such a way as to exploit the large optical domain bandwidth afforded by multiple-wavelength signals, while also preserving chip space so that the scalability of the network is not hindered. Here, we report simultaneous operation of four microring resonator modulators, each at 4 Gbps, acting on four separate wavelength channels in an optical signal resulting in an overall transmission capacity of 16 Gbps. Furthermore, all four wavelengths are modulated in a single silicon waveguide, creating a direct, space-efficient conversion from space-parallel electronics to wavelength-parallel optics.

## 2. Direct Translation with Microring Modulators

Ring modulators have been explored in depth [1-5] and single-wavelength operation of SOI microring modulators has been demonstrated [4,5]. This device, like former ones reported, operates based on the free carrier plasma dispersion effect [6]. Carriers are injected through *p-n* junctions surrounding the microring waveguides changing the index and shifting the wavelength of the rings' resonant modes. Aligning the wavelength of an optical signal near the edge of the ring's transmission spectrum results in electro-optic modulation. The four microrings contain independent *p-n* junctions, but they are each coupled to the same waveguide (Fig 1a).

Because each modulator affects only lightwaves which exist within a very small spectral range, this design provides a host of advantages over other combinations of modulators and multiplexers. First, since the signals do not need to be demultiplexed and multiplexed before and after modulation, no couplers, polarizers, or gratings are required on the chip; the signals share the same waveguide during this process. Therefore, the optical losses are reduced to the simple propagation losses of the lightwave passing through the waveguide, and space is conserved, not only by the compact microring modulators, but also by the omission of the unnecessary passive components. Also, the electrical connections can be directed in parallel to several rings along a single waveguide, rather than dividing the components of an electrical bus across non-adjacent regions of the PIC, which could result in timing problems or electrical losses.

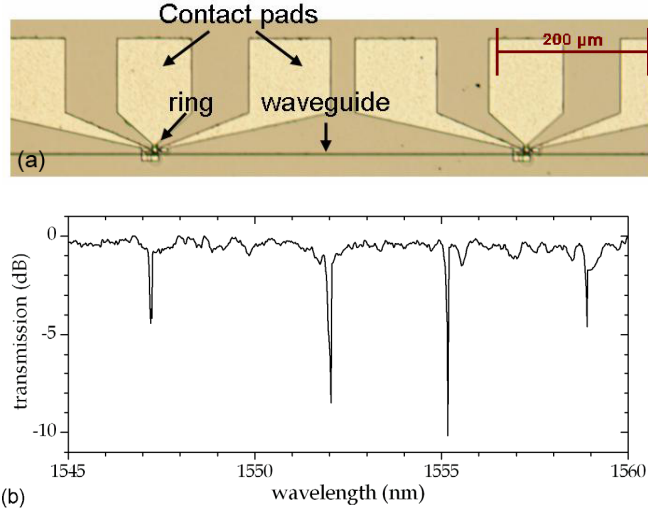


Fig. 1. (a) Image of two of the four microring modulators and (b) a transmission spectrum of the waveguide coupled to the four microrings with no bias applied.

### 3. Device and Experimental Setup

The tested device is made up of an SOI waveguide coupled to four microrings in series, which were designed with 4.98, 5.00, 5.02, and 5.04  $\mu\text{m}$  radii (Fig. 1a). The full-widths at half-maximum (FWHMs) of the four rings' transmission spectra are all approximately 0.1 nm (Fig. 1b). The experimental setup (Fig. 2a) involves four tunable lasers with independent polarization controllers, multiplexed onto a single fiber and inserted into an EDFA. The continuous wave light is coupled to an SOI waveguide where it traverses a number of bends before encountering the microrings (Fig. 2b). As the modulated, wavelength-parallel signal exits the chip, it passes through a polarizer before being collected in a fiber. At this point the signal is inserted into another EDFA; a wavelength-tunable filter then selects one wavelength channel from the multiple-wavelength signal for analysis. A high speed receiver sends the detected electrical signal to a bit error rate (BER) tester and oscilloscope. In order to drive the ring modulators, a pulse pattern generator (PPG) supplies four electrically-decorrelated 4-Gbps NRZ-OOK signals encoded with a 2<sup>7</sup>-1 PRBS. The parallel electronic signals receive amplification and DC bias adjustments before being introduced to the contact pads through RF probes. A 4-GHz clock signal synchronizes the BER tester with the PPG for error assessment.

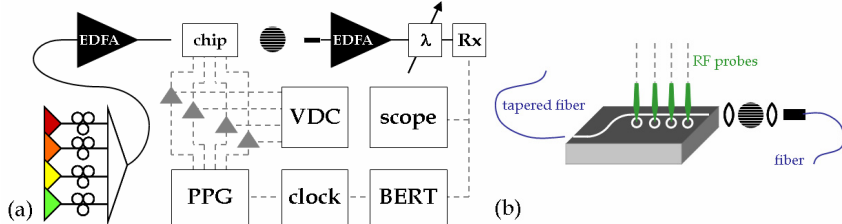


Fig. 2. Schematic of the (a) experimental setup and (b) chip interface with fiber (solid) and electrical (dashed) connections shown. Components include multiplexed lasers (colored triangles) with independent polarization controllers, polarizer (gray circle), lenses and fiber collimator, EDFA, wavelength-tunable grating filter ( $\lambda$ ), high-speed receiver (Rx), oscilloscope (scope), BER tester (BERT), clock generator, pulse pattern generator (PPG), DC voltage supply (VDC), and high-speed voltage amplifiers with bias tee circuits (gray triangles).

### 4. Experimental Results

For each of the four modulated optical signals, error free operation ( $\text{BER} < 10^{-12}$ ) at 4 Gbps was observed. In addition, Q factor extrapolations were performed for each of the four signals [7]. Since it is sometimes not feasible to measure the BER of extremely high quality signals, the Q factor may be approximated through a linear extrapolation of data obtained from BER window measurements. The sampling window widths and heights that provided BERs of  $10^{-2}$ ,  $10^{-3}$ ,  $10^{-4}$ ,  $10^{-5}$ ,  $10^{-6}$ ,  $10^{-7}$ ,  $10^{-8}$ , and  $10^{-9}$  were recorded. Then, the Q factors, obtained from the BERs using [8], were plotted against the widths (Fig. 3a) and heights (Fig. 3b) of the sampling windows. An extrapolation of the Q factor to the optimal decision threshold, where the window is equal to zero, is used to quantify the signal integrity. The extrapolated Q factors with confidence margins (and approximate BERs) for the four optical signals from lowest to highest wavelength are:  $8.2 \pm$

$0.26 (10^{-16})$ ,  $9.0 \pm 0.95 (10^{-19})$ ,  $7.9 \pm 0.61 (10^{-15})$ , and  $10.3 \pm 2.07 (10^{-25})$ . All four wavelengths are limited by the time extrapolation, rather than the amplitude. The minor variation between the extrapolated Q factors of the three lowest wavelengths is most likely due to small differences in the resonator lineshapes [5]. This is seen most drastically in the degraded slope of the lowest wavelength extrapolation (darkest), which exhibits some slight double-peak features in the transmission spectrum, and has the lowest extinction ratio of the four signals. The significantly larger Q factor at 1560.37 nm (lightest) is a result of its location furthest from the noise spectra of the two EDFA used in the experimental setup. Since the EDFA were required only to overcome the fiber-to-chip and chip-to-fiber coupling losses, modulators in future exclusively on-chip networks may display even better signal quality where amplification is not required.

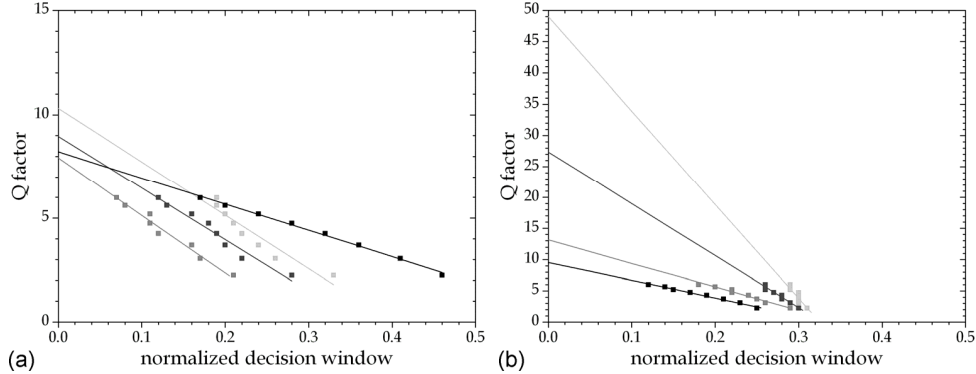


Fig. 3. Linear Q factor extrapolations from (a) time and (b) amplitude measurements for the four modulated signals. The measured Q factor (■) is plotted against the fraction of the eye diagram's sampling window with linear extrapolations (lines) shown. From darkest to lightest the curves represent 1547.78, 1552.88, 1556.02, and 1560.37 nm.

## 5. Conclusions

We have shown simultaneous, error-free operation of four microring modulators acting on a WDM signal in a single SOI waveguide. Q factor extrapolations were used to characterize the signal integrity. The topology of this modulator design is particularly favorable as a transparent translator from an electrical bus to a multiple-wavelength optical signal. This conversion process is a key element of high-bandwidth interconnects based on PICs, which can potentially be used in inter- and intra-chip networks, so that the highly parallel electronic data generated from processor cores are encoded onto multiple-wavelength optical signals in a power efficient manner that preserves both bandwidth and chip area.

K. Bergman, B.G. Lee, B.A. Small, and J.D. Foster would like to acknowledge the support of the National Science Foundation under contract CCF-0523771. M. Lipson and Q. Xu acknowledge that this work has been partially carried out as part of the Interconnect Focus Center Research Program at Cornell University, supported in part by the Microelectronics Advanced Research Corporation (MARCO) and its participating companies.

## 6. References

- [1] M. Lipson, "Guiding, modulating, and emitting light on silicon—challenges and opportunities," *J. Lightw. Technol.*, vol. 23, no. 12, pp. 4222-4238, Dec 2005.
- [2] P. Rabiei, W.H. Steier, C. Zhang, L.R. Dalton, "Polymer micro-ring filters and modulators," *J. Lightw. Technol.*, vol. 20, no. 11, pp. 1968-1975, Nov 2002.
- [3] H. Tazawa, W.H. Steier, "Analysis of ring resonator-based traveling-wave modulators," *IEEE Photon. Technol. Lett.*, vol. 18, no. 1, pp. 211-213, Jan 2006.
- [4] Q. Xu, B. Schmidt, S. Pradhan, M. Lipson, "Micrometre-scale silicon electro-optic modulator," *Nature*, vol. 435, pp. 325-327, May 2005.
- [5] Q. Xu, B. Schmidt, J. Shakya, M. Lipson, "Cascaded silicon micro-ring modulators for WDM optical interconnection," *Opt. Express*, vol. 14, no. 20, pp. 9430-9435, Oct 2006.
- [6] R.A. Soref, B.A. Bennett, "Electrooptical effects in silicon," *IEEE J. Quantum Electron.*, vol. 23, no. 1, pp. 123-129, Jan 1987.
- [7] N. S. Bergano, K. W. Kerfoot, C. R. Davidson, "Margin measurements in optical amplifier systems," *IEEE Photon. Technol. Lett.*, vol. 5, no. 3, pp. 304-306, Mar 1993.
- [8] B.A. Small, T. Kato, K. Bergman, "Measurements of very low bit error rates for an optical packet switching node," *IEEE Photon. Technol. Lett.*, vol. 17, no. 11, pp. 2379-2381, Nov 2005.